

Published in final edited form as:

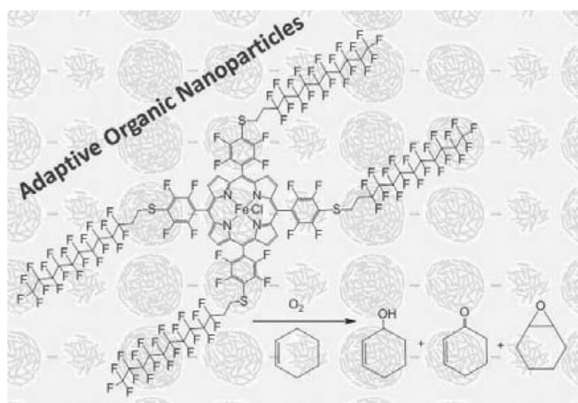
Macromol Rapid Commun. 2012 July 26; 33(14): 1220–1226. doi:10.1002/marc.201200107.

Adaptive Organic Nanoparticles of a Teflon-Coated Iron (III) Porphyrin Catalytically Activate Dioxygen for Cyclohexene Oxidation

Amit Aggarwal, Sunaina Singh, Jacopo Samson, and Charles Michael Drain*

Department of Chemistry and Biochemistry, Hunter College and Graduate Centre of the City University of New York, NY 10065, USA

Abstract



Self-organized organic nanoparticles (ONP) are adaptive to the environmental reaction conditions. ONP of fluorinated alkyl iron(III) porphyrin catalytically oxidize cyclohexene to the allylic oxidation products. In contrast, the solvated metalloporphyrin yields both allylic oxidation and epoxidation products. The ONP system facilitates a greener reaction because about 89% reaction medium is water, molecular oxygen is used in place of synthetic oxidants, and the ambient reaction conditions used require less energy. The enhanced catalytic activity of these ONP is unexpected because the metalloporphyrins in the nanoaggregates are in the close proximity and the TON should diminish by self-oxidative degradation. The fluorinated alkyl chain stabilizes the ONP toward self-oxidative degradation.

Keywords

catalyst; dynamic light scattering; metalloporphyrin; organic nanoparticles; oxidation; green chemistry

Supporting Information

Supporting Information is available from the Wiley Online Library or from the author.

1. Introduction

Allylic oxidation of olefins is a key organic transformation in a variety of synthetic strategies such as for steroids, and is often carried out using toxic metal oxidants as reagents or as catalysts. A variety of transition metal-based catalysts such as Cr, ^[1] Rh, ^[2] Mn, ^[3] Ru, ^[4] and Se ^[5] are reported but have different problems such as cost, scope, complete removal of the metal, and synthesis. From an environmental and cost-effective viewpoint, catalytic oxidation processes employing molecular oxygen, in aqueous media, and under ambient conditions are extremely valuable. Recently, Zhao and Yeung ^[6] reported the use of PhI(OAc)₂ and *t*BuOOH reagents to generate the *t*BuO• radical to yield α , β -unsaturated enones in good yield and regioselectivity. Ammonium hypoiodite catalysis is another example of metal-free oxidation. ^[7]

Metalloporphyrins are an important class of organic molecules because of their tunable optical, photophysical, and chemical properties that enable a wide range of applications such as photonics, therapeutics, and catalysts. Various metalloporphyrins with Fe, Mn, Co, and other metal ions have been studied and used as catalysts in laboratory-scale reactions using a variety of oxygen sources. ^[8] These reactions can model the activity of cytochrome P₄₅₀ monooxygenation reactions. ^[9] The catalytic activity of metalloporphyrins depends on the structure of the porphyrin, the central metal atom, the source of oxidant, solvent, the nature of axial ligand, temperature, pressure, and the structure of the substrate. ^[8]

Self-oxidative degradation during the catalytic process is a key issue that limits use of metalloporphyrin catalysts. ^[8a] To overcome this, electron withdrawing groups such as Cl and F, or bulky substituents are often appended to the porphyrin macrocycle. ^[10] Supramolecular porphyrin catalysts are designed to prevent self-oxidative degradation and to enhance substrate selectivity and/or regioselectivity. ^[11] A variety of oxygen donors such as peracids, iodosylbenzene, peroxides, monopersulfates, and molecular oxygen are used for these reactions. ^[8a] In many ways, activation of molecular oxygen in air is preferable because it is cheap, readily available, and a greener reagent in that there is no energy used to manufacture and store it.

The use of inorganic nanomaterials composed of metal atoms, metal oxides, and composites have been well explored for a range of application such as catalysts. ^[12] However, the formation and activity of organic nanomaterials are more recent, and porphyrinoids are at forefront of this research because of their remarkable photochemical and catalytic properties, stability, and ease of preparation. ^[13] This work builds upon the principles of supramolecular chemistry as a versatile avenue for advanced functional materials. Hupp and co-workers, ^[11a, 14] for example, reported a self-assembled (discrete) metalloporphyrin catalyst formed from different porphyrinoids can be robust and have enhanced catalytic activity over the corresponding metalloporphyrin in solution. ^[11a, 14]

Supramolecular organic nanoparticles (ONP) of porphyrinoids are self-organized (non-discrete) systems formed via noncovalent interactions. ^[13b, 15] Because ONP are dynamic so can adapt to environmental changes, ONP are fundamentally different from inorganic nanomaterials. The formation of ONP of porphyrins was discussed previously and is generally accomplished by adding a concentrated solution of the porphyrin to a miscible nonsolvent with a few percent of a triethyleneglycol monomethylether glycol (PEG₁₆₄) while vigorously mixing. ^[13a] Stabilization of the suspension of ONP to precipitation is effected by the small quantities of the PEG in the solvent system. We previously reported the effects of various conditions on the formation, size, and stability of porphyrinic ONP. For example, in addition to the specific molecular structure of the porphyrin, the molecular weight and quantity of PEG stabilizer, the ratio of host to guest solvents, temperature, and

type of mixing all factor in the size, stability and morphology of ONP.^[13b] Though the specific preparative methods depend on the molecular structure (such as free base, metal ion, and exocyclic moieties), the conditions can be varied to afford ONP of different sizes.^[13b, 16] For 5,10,15,20-tetrakis-[4-(1'H,1'H,2'H,2'H-heptadecafluorodecane-1-thiol)-2,3,5,6-tetrafluorophenyl]porphyrinato iron(III) chloride, [Fe(III)TPPF₈₄]Cl, the particle size can be tuned by increasing in the volume of the PEG₁₆₄, but without stabilizer no ONP formation was observed by dynamic light scattering (DLS) and UV-visible spectroscopy and the metalloporphyrin rapidly and quantitatively precipitates. The size and internal structure of porphyrinic nanoparticles depend on: (a) the nature and magnitude of intermolecular forces between the various components, for example, the porphyrin, host and guest solvents, and the stabilizer; (b) the ratio of the host to guest solvent, (c) the type of mixing, and (d) the nature of peripheral substituents on the porphyrin and chelated metal ion.^[13c] These ONP are stable for many weeks at 4 °C, and ONP of catalytically active metalloporphyrins are generally more efficient catalysts than the component molecule in solution.^[13c]

Previously, we reported that 10 nm diameter ONP of Fe(III)TPPF₂₀ (Scheme 1) have about 10-fold enhanced catalytic activity for the allylic oxidation of cyclohexene to yield the α , β -unsaturated ketone and alcohol (Scheme 2) under ambient conditions, and using molecular oxygen as oxidant.^[13c] Conversely, the epoxide (Scheme 2) is the only product from the completely solvated metalloporphyrin in organic solvents, and synthetic oxygen sources such as H₂O₂ are required. During both catalytic processes, the porphyrin decomposes completely. The objective of the present study is to evaluate the catalytic activity of ONP of a metalloporphyrin bearing fluoruous alkanes designed to increasing the stability toward self-oxidative degradation.

Our hypothesis was that appending fluoruous alkanes to the macrocycle would increase metalloporphyrin stability by inhibiting cofacial interactions. Indeed, [Fe(III)TPPF₈₄]Cl (Scheme 1) is found to be more stable toward self-oxidative degradation, but the overall yields of the α , β -unsaturated ketone and alcohol are less than ONP of [Fe(III)TPPF₂₀]Cl.

2. Experimental Section

The Fe(III)TPPF₈₄ catalyst was prepared according to our previous report,^[17] wherein 3,3,4,4,5,5,6,6,7,7,8,8,9,9,10,10,10-heptadecafluoro-1-decanethiol was reacted with the perfluorophenylporphyrin, [Fe(III)TPPF₂₀]Cl, in DMF with N,N-diisopropylethylamine for 15 min under a N₂ atmosphere (Scheme 1, see Supporting Information). All spectral data are consistent with the structure (Figure S1 and S2, Supporting Information). The nanoparticles of Fe(III)TPPF₈₄ were prepared similar to our previous report on the formation of ONP of the other porphyrinoids. 0.4 mL of a 1×10^{-3} M stock solution of Fe(III)TPPF₈₄ in THF was mixed with 0.2 mL of PEG₁₆₄ in a 10.0 mL vial and 5.0 mL nanopure water was then added over 60 s while sonicating and then the solution was further sonicated for another 2–3 min.^[13a-c] The ONP were characterized by UV-visible spectroscopy and DLS. The average diameter of the ONP of Fe(III)TPPF₈₄ is 15–20 nm (Figure S3 and S4, Supporting Information). The aggregation of the metalloporphyrins in the nanoscaled particles was also confirmed by the broadening of the Soret and Q bands as discussed previously.^[13b, c] The broadening is due to edge-to-edge (J) and face-to-face (H) aggregation of the dyes in the ONP.

2.1. Catalytic Oxidation of Cyclohexene

The catalytic activity for the oxidation of cyclohexene by Fe(III)TPPF₈₄ in solution and as supramolecular ONP was explored here. We used the $\approx 21\%$ O₂ in air, pure O₂, and 30% H₂O₂, as oxidants. The metalloporphyrin was the limiting reagent and the reactions run

exhaustively in all the reactions to assure accurate comparisons in turnovers in systems that have different activities (rates). Reactions were run for 24 h and then were quenched in an ice bath. Twenty microliters of toluene were used as internal standard and then 2 μL of the diluted solution was then injected into an Agilent 5975 series GC-MS for analysis of the oxidation products of cyclohexene (see Supporting Information). All reactions were stirred using a magnetic stirring bar and were run a minimum of four times and the reported data represents the average of these reactions.

3. Results and Discussion

The preparation and use of metalloporphyrin ONP catalysts has several advantages: ease of preparation, use of water as an eco-friendly solvent, avoids hazardous chemicals such as halogenated solvents or toxic catalysts, and reduces the energy requirement because the reactions runs at ambient temperature and pressure.

Cyclohexene is widely used as a standard substrate to study the catalytic activity of various metalloporphyrins using a variety of oxidizing agents and conditions.^[18] The formation of different products or product ratios depends on the catalytic system. The possible products for cyclohexene oxidation are cyclohexenoxide, and the allylic substitution products: 2-cyclohexene-1-ol and 2-cyclohexene-1-one (Scheme 2).

The catalytic activity of ONP of Fe(III)TPPF₈₄ using pure oxygen, H₂O₂, and $\approx 21\%$ O₂ in air as oxidizing agents is discussed. The highly fluorinated alkyl groups on the para-positions of the meso tetrafluorophenyl groups in Fe(III)TPPF₈₄ increase the stability of the metalloporphyrin toward self-oxidative degradation, but render the system less catalytically active under these conditions.

3.1. Solution Phase Catalysis by Fe(III)TPPF₈₄

In solution, the Fe(III)TPPF₈₄ catalyst activates O₂ for the oxidation of cyclohexene in CH₃OH: CH₃CN (1:3) to yield all three products, epoxide:enol: enone = 1:1.5:3 (Scheme 2, Table 1). This activity is in contrast to Fe(III)TPPF₂₀, which requires H₂O₂, does not activate O₂, and yields only the epoxidation product.^[19] The rate of the former reaction is slow compared with the latter. For the Fe(III)TPPF₈₄ solution phase reaction, both solubilized metalloporphyrin and a small amount of large aggregates (≈ 1100 nm diameter) were observed by DLS but are not obvious with UV–visible spectroscopy. The formation of the allylic oxidation products along with the epoxide reflects this observation. The TON is defined as the total amount of products formed per porphyrin molecule. UV–visible analysis of the reaction mixture after the reaction was run exhaustively shows $\approx 36\%$ porphyrin remains (Figure S5, Supporting Information). Increased concentration of cyclohexene in these reactions increases the TON (Figure 1). The highly fluorinated alkyl chains moieties dramatically increase the stability toward self-oxidation compared with [Fe(III)TPPF₂₀]Cl, which is more stable than the nonfluorinated compound.^[19] When H₂O₂ is used as the oxidizing agent, even halogenated metalloporphyrins undergo complete decomposition in a few minutes during the olefinic oxidation catalysis.^[19]

The reduced activity and enhanced stability may arise from the long fluorinated alkyl chains folding back over the metalloporphyrin faces, driven by hydrophobic effects and intermolecular interactions among the fluorinated groups. The shielding of the reactive face may also decrease access of the hydrocarbon substrate. The increased solubility of O₂ in fluorinated phases may also contribute to the observed activity of Fe(III)TPPF₈₄. Reactions run for up to 72 h have the same ratio of products and TON, but the porphyrin is completely decomposed. Recharging the reaction after 24 h by providing more oxygen is no more efficacious than the 72 h reaction. Reactions run under elevated temperature and pressure

also result in complete decomposition of the porphyrin, gives similar oxidation product ratios, but with a reduced TON (Table 1). The increased rate of catalyst decomposition and decreased TON may be because the elevated T increases the dynamics of the fluorinated alkyl chains to expose the macrocycle to approach of another Fe(III)TPPF₈₄ (Figure S6, Supporting Information). Changing the reaction solvent to ethanol/toluene (1:3) quenches the reaction using O₂. Addition of anthracene to the reaction mixture can increase the catalytic activity of metalloporphyrins,^[14a] but did not effect the Fe(III)TPPF₈₄ reaction. No cyclohexene oxidation products were observed when the reactions used H₂O₂, but the catalyst decomposes in ≈15 min. The ≈21% O₂ in air is not effective in solution phase reaction. Note that the nonfluorinated analogue, the dodecanethiol adduct (R =C₁₂H₂₅S-), is catalytically inactive and no porphyrin decomposition was observed.

The initial metalloporphyrin oxidation products, speculated to be the porphyrin radical cation formed from an intramolecular metal ion macrocycle electron transfer,^[20] are more readily oxidized such that once the macrocycle opens, and is trapped in the ONP, it further oxidizes to as yet unidentified products. The UV–visible analysis of the reaction mixture before and after the reaction does not detect porphyrin oxidation intermediates such as chlorin, isobacteriochlorin, bacteriochlorin, bilirubin, or dipyrromethane. All of these compounds are known and have specific peaks in the UV–visible spectrum. GC–MS data do not show significant amounts of compounds >50 amu.

3.2. Catalysis by Nanoparticles of Fe(III)TPPF₈₄

The 15–20 nm diameter ONP of Fe(III)TPPF₈₄ are more catalytically active than the solvated metalloporphyrin. These ONP oxidize cyclohexene using O₂ to yield only the allylic oxidation products, 2-cyclohexene-1-one and 2-cyclohexene-1-ol with a trace amount of epoxide (Scheme 2) at about a fourfold greater TON (Table 1).

UV–visible spectra of reaction mixtures after a 24 h reaction show that ≈26% of the porphyrin remains, but eventually Fe(III)TPPF₈₄ decomposes after longer reaction times (Figure S7, Supporting Information). Intermediate oxidation products for the metalloporphyrin decomposition, such as chlorin, isobacteriochlorin, bacteriochlorin, bilirubin, or dipyrromethane were not observed by UV– visible analysis of the reaction mixture during the course of the reaction. Though the allylic oxidation products for ONP of Fe(III)TPPF₈₄ is consistent with our previous report on Fe(III)TPPF₂₀ ONP,^[13c] and the catalytic activity is less, but they are more robust toward self-oxidative degradation. Fe(III)TPPF₈₄ ONP are inactive with other oxidants such as the ≈21% O₂ in air and H₂O₂. ONP of the hydrocarbon analogue are inactive under the same conditions. Kinetic assays indicate that the nanoparticles have very low or almost no activity during the first few hours of the reaction. GC–MS analysis of the reactions mixture for different time intervals for first few hours shows no oxidation product for cyclohexene. Also, UV–visible spectra indicate no degradation of ONP for the first few hours of the reactions. After 8–10 h of reaction time, we see a noticeable conversion of cyclohexene and then this saturates after about 20 h (Figure S8, Supporting Information).

3.3. Internal Organization of the ONP

The detailed structural organization of the porphyrins inside the ONP remains unknown because the intermolecular forces, which hold these molecules into nanoaggregates are weak, nonspecific, and reversible.^[13b, c] The organization of the metalloporphyrins in the ONP strongly depends on the structure of component molecule, nature and ratio of host–guest solvent, stabilizer used, the mode of preparation, and temperature. We^[13b, c] and others^[21] found that the ONP may contain a number of subdomains of porphyrins and the solvent–stabilizer filled voids or channels of unknown size and distribution.

Because of the supramolecular interactions, the organization of the ONP is also adaptive in that it responds to the presence of substrates. Our group previously examined a number of ONP of porphyrins and metalloporphyrins using UV–visible and DLS in solution, and compared this to atomic force microscopy (AFM) studies of the ONP cast on the surfaces. AFM studies of nanoparticles of porphyrins cast on surfaces do not always show same size as in solution because of the surface energetics and the adaptive properties of the ONP.^[13a,b,22] There is no a priori correlation between particle size and structure in solution with the morphology on surfaces. On hydrophobic surfaces, ONP of some metalloporphyrins disaggregate to reveal the constituent subdomains.^[23] TEM characterization of ONP of Fe(III)TPPF₈₄ shows a range of particle sizes. The 25–30 nm cluster in Figure 2 consists of 3–4 ONP from the cast solution. The DLS give a hydrodynamic diameter of 15–20 nm (Figure S4, Supporting Information). The observed aggregation of 3–4 of the 15–20 nm diameter ONP on the grid as the solvent evaporates is typical for these types of systems. The TEM also shows that the 15–20 nm diameter ONP are composed of smaller particles corresponding to the subdomains. The histogram in Figure 2 shows the size distribution for the subdomains on the grid and is consistent with the presence of dimers or trimers of the metalloporphyrins.

3.4. Mechanism

The mechanism for metalloporphyrin-catalyzed olefinic oxidation reactions have been well reviewed and depends on the specific compounds used. One main mechanism is H-atom abstraction.^[19, 24] The aggregation of metalloporphyrins in the ONP may facilitate oxo-bridge complex formation, which is known to effect catalytic activity.^[8a] Formation of allylic oxidation products by the ONPcatalyzed reaction suggest that the reaction goes through a different mechanistic pathway than when the epoxide is formed. The oxidation by the ONP may proceed through a radical mechanism.^[13c] One plausible explanation for the slow reactivity and increased TON for these ONP catalytic reactions may be that only the outer layer of the metalloporphyrins in the nanoaggregates is available for the initial oxidative process. When the porphyrins in the outer layer eventually decompose, they fall off to expose the next active layer. The onion type was recently discussed,^[13c] and is consistent with the DLS data that show that the size of the ONP decreases as the reaction progresses (Figure S12, Supporting Information). The higher ratio of ketone than alcohol for these ONP catalytic reactions may be because the initially formed alcohol gets further oxidized to ketone before it escapes the ONP cage. As cyclohexene is hydrophobic and the reaction solvent is mostly water, the substrate rapidly partitions into the ONP as indicated by the change in color of ONP and shift in the UV–visible spectral peaks. The organization of the metalloporphyrins within the ONP can change with the binding of the substrate.^[13f] Thus, the mechanism has three convolved components in terms of the ONP. (1) The fundamental chemical reactivity in terms of the metalloporphyrin, substrate, solvent, temperature, and axial ligands; as extensively studied previously. (2) The role of the aggregation of the metalloporphyrins in the ONP in facilitating oxo-bridge formation, slowing down the reaction, and taking up the substrate from the mostly aqueous solution. (3) The nanoarchitecture of the aggregates may limit the approach of the substrate to the metal ion active site.

4. Conclusion

Appending fluorinated alkanes onto a core Fe(III)TPPF₂₀ platform using simple, high-yield chemistry affords a robust catalyst that can activate O₂ for allylic oxidations. Although these adaptive ONP of Fe(III)TPPF₈₄ exhibit reduced activity compared with the ONP of the Fe(III)TPPF₂₀ platform, this strategy to make porphyrin derivatives provides a testbed to examine a plethora of other porphyrin derivatives and substrates for diverse

applications.^[16, 25] The porphyrin ONP catalysis reported herein represents a model for the green chemistry because $\approx 89\%$ of the reaction solvent is water, halogenated solvents are avoided, and O_2 is used as the oxidant. Allylic oxidation reactions are widely used in many areas of organic synthesis ranging from agricultural products to pharmaceuticals, and these ONP systems avoid use of reagents such as SeO_2 and other metal oxides.^[26] New high-yield synthetic methods may make simple metalloporphyrins attractive use of porphyrin catalysts on larger scales,^[25a, 27] for example, in solvent-free reactions.^[28] These studies suggests that all catalytic reactions using compounds such as metalloporphyrinoids should be examined for the presence of nanoparticles or aggregates because ONP can be much more active than the compounds in solution, thereby dominating the observed activity.

Supplementary Material

Refer to Web version on PubMed Central for supplementary material.

Acknowledgments

Supported by the National Science Foundation (NSF) CHE-0847997 to C.M.D. Hunter College Chemistry infrastructure is supported by the NSF, National Institutes of Health including the RCMI program (G12-RR-03037 and 8 G12 MD007599), and the City University of New York.

References

1. Muzart J. *Chem. Rev.* 1992; 92:113.
2. a) Choi H, Doyle MP. *Org. Lett.* 2007; 9:5349. [PubMed: 18027961] b) Doyle MP. *J. Org. Chem.* 2006; 71:9253. [PubMed: 17137350]
3. Shing TKM, Yeung Y-Y, Su PL. *Org. Lett.* 2006; 8:3149. [PubMed: 16805574]
4. Harre M, Haufe R, Nickisch K, Weinig P, Weinmann H, Kinney WA, Zhang X. *Org. Proc. Res. Dev.* 1998; 2:100.
5. Crich D, Zou Y. *Org. Lett.* 2004; 6:775. [PubMed: 14986972]
6. Zhao Y, Yeung Y-Y. *Org. Lett.* 2010; 12:2128. [PubMed: 20387842]
7. Uyanik M, Okamoto H, Yasui T, Ishihara K. *Science.* 2010; 328:1376. [PubMed: 20538945]
8. a) Meunier B. *Chem. Rev.* 1992; 92:1411. b) Costas M. *Coord. Chem. Rev.* 2011; 255:2912.
9. a) Silaghi-Dumitrescu R. *J. Biol. Inorg. Chem.* 2004; 9:471. [PubMed: 15106002] b) Meunier B, de Visser SP, Shaik S. *Chem. Rev.* 2004; 104:3947. [PubMed: 15352783] c) Newcomb M, Hollenberg PF, Coon MJ. *Arch. Biochem. Biophys.* 2003; 409:72. [PubMed: 12464246] d) Chandrasena REP, Vatsis KP, Coon MJ, Hollenberg PF, Newcomb M. *J. Am. Chem. Soc.* 2004; 126:115. [PubMed: 14709076]
10. a) Poltowicz J, Pamin K, Haber J. *J. Mol. Catal. A: Chem.* 2006; 257:154. b) Arasasingham RD, He GX, Bruice TC. *J. Am. Chem. Soc.* 1993; 115:7985. c) Ellis PE Jr, Lyons JE. *Coord. Chem. Rev.* 1990; 105:181.
11. a) Lee JY, Farha OK, Roberts J, Scheidt KA, Nguyen ST, Hupp JT. *Chem. Soc. Rev.* 2009; 38:1450. [PubMed: 19384447] b) Shultz AM, Farha OK, Hupp JT, Nguyen ST. *J. Am. Chem. Soc.* 2009; 131:4204. [PubMed: 19271705]
12. a) Bao J, Chen W, Liu T, Zhu Y, Jin P, Wang L, Liu J, Wei Y, Li Y. *ACS Nano.* 2007; 1:293. [PubMed: 19206679] b) Huang Y, Ma W, Li J, Cheng M, Zhao J, Wan L, Yu JC. *J. Phys. Chem. B.* 2003; 107:9409.
13. a) Gong X, Milic T, Xu C, Batteas JD, Drain CM. *J. Am. Chem. Soc.* 2002; 124:14290. [PubMed: 12452687] b) Drain CM, Smeureanu G, Patel S, Gong X, Garno J, Arijeloye J. *New J. Chem.* 2006; 30:1834. c) Smeureanu G, Aggarwal A, Soll CE, Arijeloye J, Malave E, Drain CM. *Chem. Eur. J.* 2009; 15:12133. [PubMed: 19777510] d) Cho K, Kerber WD, Lee SR, Wan A, Batteas JD, Goldberg DP. *Inorg. Chem.* 2010; 49:8465. [PubMed: 20735145] e) Qiu Y, Chen P, Liu M. *J. Am. Chem. Soc.* 2010; 132:9644. [PubMed: 20578772] f) Aggarwal A, Qureshy M, Johnson J, Batteas JD, Drain CM, Samaroo D. *J. Porphyrin Phthalocyanine.* 2011; 15:338.

14. a) Merlau ML, Cho S-H, Sun S-S, Nguyen ST, Hupp JT. *Inorg. Chem.* 2005; 44:5523. [PubMed: 16022551] b) Lee SJ, Hupp JT. *Coord. Chem. Rev.* 2006; 250:1710.c) Merlau ML, Mejia Md P, Nguyen ST, Hupp JT. *Angew. Chem. Int. Ed.* 2001; 40:4239.
15. a) Wang Z, Medforth CJ, Shelnutz JA. *J. Am. Chem. Soc.* 2004; 126:16720. [PubMed: 15612699] b) Wang Z, Medforth CJ, Shelnutz JA. *J. Am. Chem. Soc.* 2004; 126:15954. [PubMed: 15584716]
16. Drain CM, Bazzan G, Milic T, Vinodu M, Goeltz JC. *Isr. J. Chem.* 2005; 45:255.
17. Varotto A, Todaro L, Vinodu M, Koehne J, Liu G-y, Drain CM. *Chem. Commun.* 2008:4921.
18. a) Kameyama H, Narumi F, Hattori T, Kameyama H. *J. Mol. Catal. A: Chem.* 2006; 258:172.b) Zhou X-T, Tang Q-H, Ji H-B. *Tetrahedron Lett.* 2009; 50:6601.c) Gharnati L, Doring M, Arnold U. *Curr. Org. Syn.* 2009; 6:342.d) Zhou X, Ji H. *Chem. Eng. J.* 2010; 156:411.
19. Stephenson NA, Bell AT. *Inorg. Chem.* 2007; 46:2278. [PubMed: 17311372]
20. Bhuyan J, Sarkar S. *Chem. Eur. J.* 2010; 16:10649. [PubMed: 20687149]
21. Kashani-Motlagh MM, Rahimi R, Kachousangi MJ. *Molecules.* 2010; 15:280. [PubMed: 20110879]
22. Xu, C. *Synthesis and Application of Organic Thin Film Modified Surfaces*, in *Chemistry*. New York: The City University of New York; 2005. p. Ph.D./.
23. a) Milic T, Garno JC, Batteas JD, Smeureanu G, Drain CM. *Langmuir.* 2004; 20:3974. [PubMed: 15969388] b) Milic TN, Chi N, Yablon DG, Flynn GW, Batteas JD, Drain CM. *Angew. Chem. Int. Ed.* 2002; 41:2117.
24. a) Arunkumar C, Lee Y-M, Lee JY, Fukuzumi S, Nam W. *Chem. Eur. J.* 2009; 15:11482. [PubMed: 19810056] b) Haber J, Matachowski L, Pamin K, Poltowicz J. *J. Mol. Catal. A: Chem.* 2003; 198:215.c) Lyons JE, Ellis PE, Myers HK. *J. Catal.* 1995; 155:59.
25. a) Drain, CM.; Singh, S. *Combinatorial Libraries of Porphyrins: Chemistry and Applications*, in *The Handbook of Porphyrin Science with Applications to Chemistry, Physics, Materials Science, Engineering, Biology and Medicine*. Kadish, K.; Smith, KM.; Guillard, R., editors. Singapore: World Scientific Publisher; 2010. p. 485b) Drain CM, Batteas JD, Flynn GW, Milic T, Chi N, Yablon DG, Sommers H. *Proc. Natl. Acad. Sci., USA.* 2002; 99:6498. [PubMed: 11880598] c) Drain CM, Nifiatis F, Vasenko A, Batteas JD. *Angew. Chem. Int. Ed.* 1998; 37:2344.d) Drain CM, Varotto A, Radivojevic I. *Chem. Rev.* 2009; 109:1630. [PubMed: 19253946] e) Jurow M, Schuckman AE, Batteas JD, Drain CM. *Coord. Chem. Rev.* 2010; 254:2297. [PubMed: 20936084] f) Radivojevic I, Varotto A, Farley C, Drain CM. *Energy Environ. Sci.* 2010; 3:1897.
26. a) Andrus MB, Lashley JC. *Tetrahedron.* 2002; 58:845.b) Crich D, Zou Y. *J. Org. Chem.* 2005; 70:3309. [PubMed: 15823003]
27. a) Drain CM, Gong X. *Chem. Commun.* 1997:2117.b) Cavaleiro, JAS.; Tomé, AC.; Neves, MGPMS. "meso-Tetraarylporphyrin Derivatives: New Synthetic Methodologies", in *The Handbook of Porphyrin Science with Applications to Chemistry, Physics, Materials Science, Engineering, Biology and Medicine*. Kadish, K.; Smith, KM.; Guillard, R., editors. Singapore: World Scientific Publisher; 2010. p. 193
28. Nia S, Gong X, Drain CM, Jurow M, Rizvi W, Qureshy M. *J. Porphyrins Phthalocyanines.* 2010; 14:621.

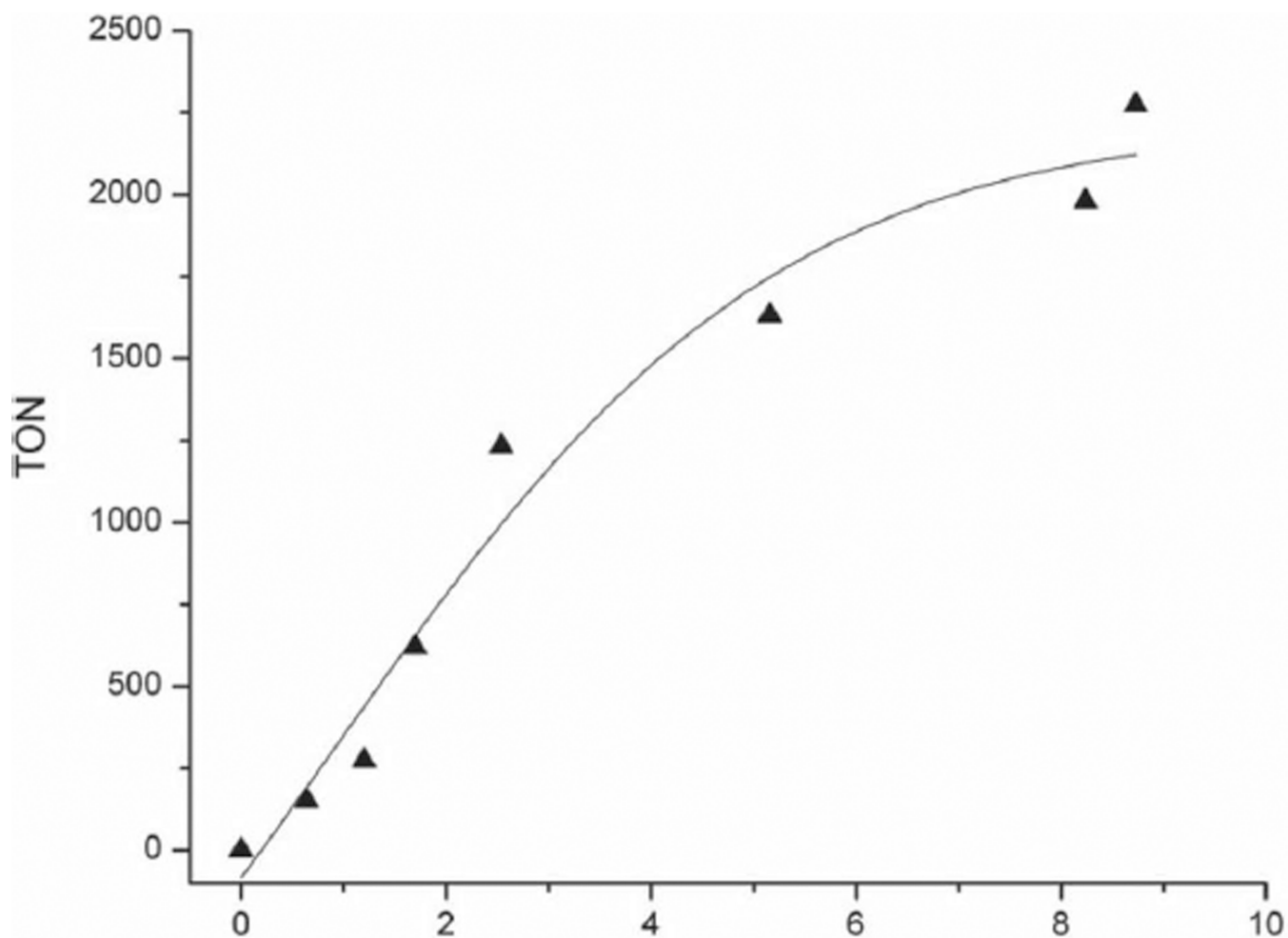


Figure 1. Catalysis of cyclohexene oxidation by Fe(III)TPPF₈₄ ONP versus TON.

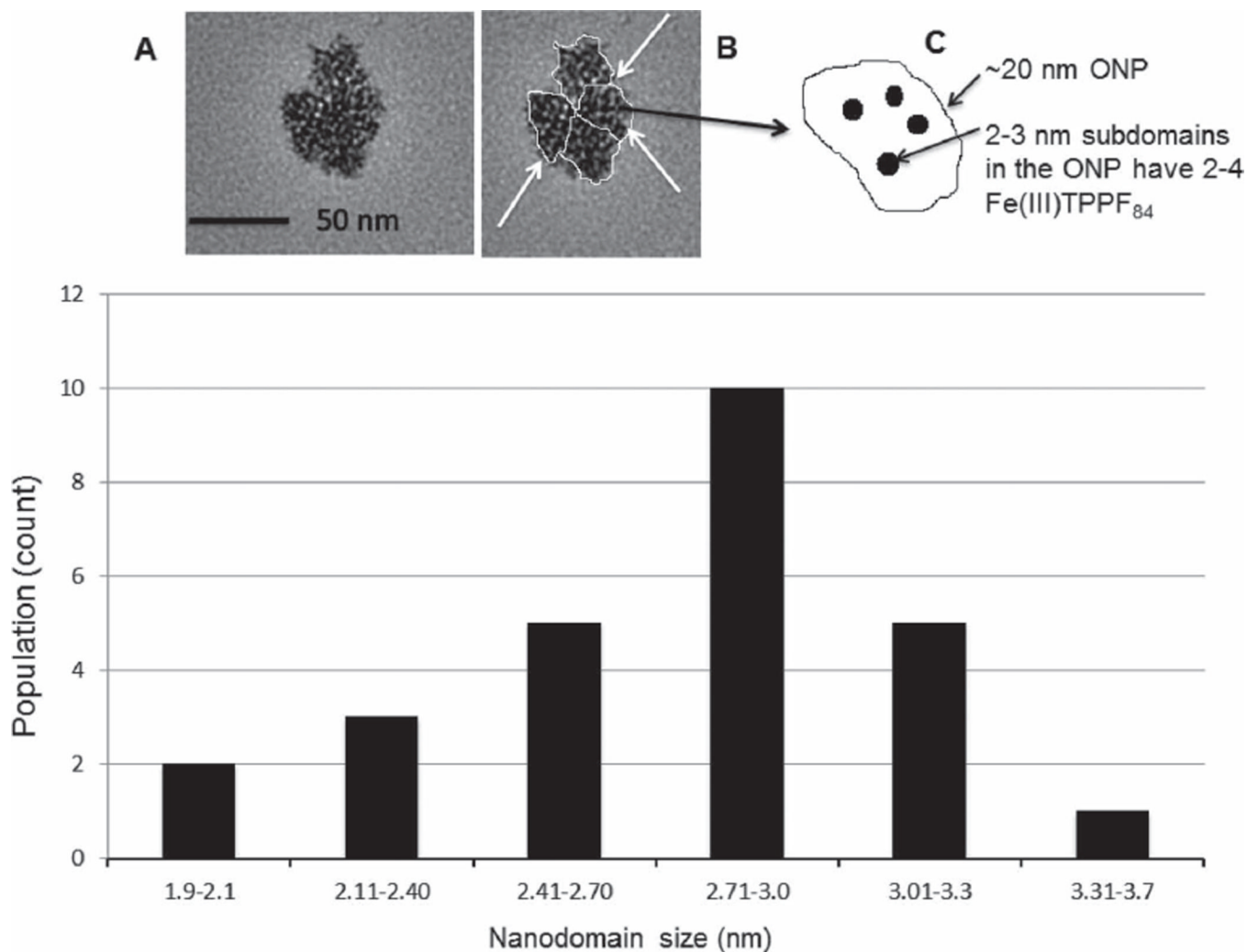
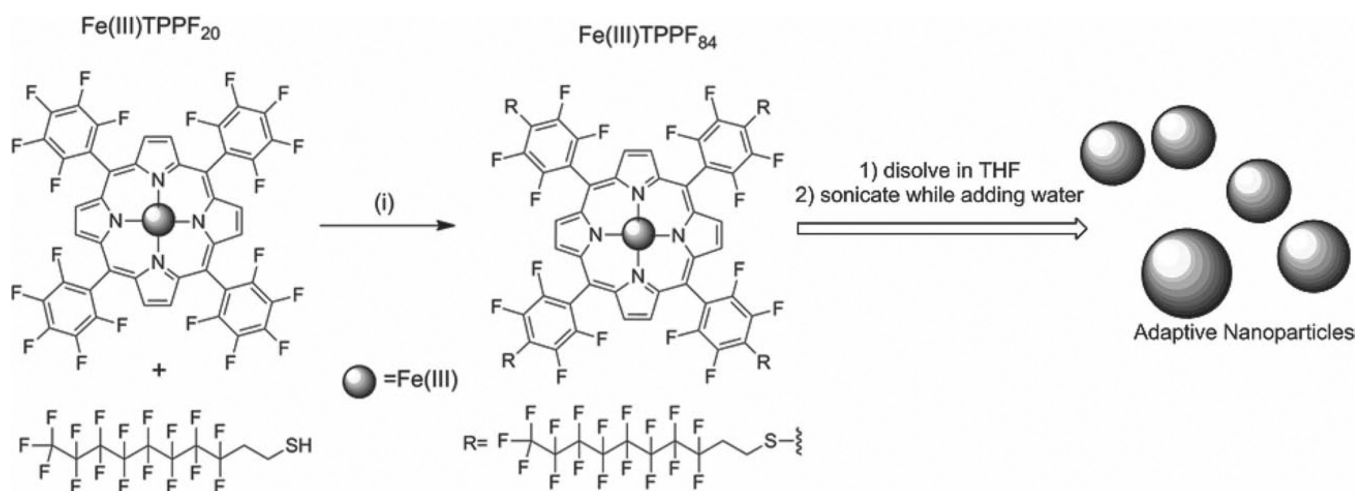
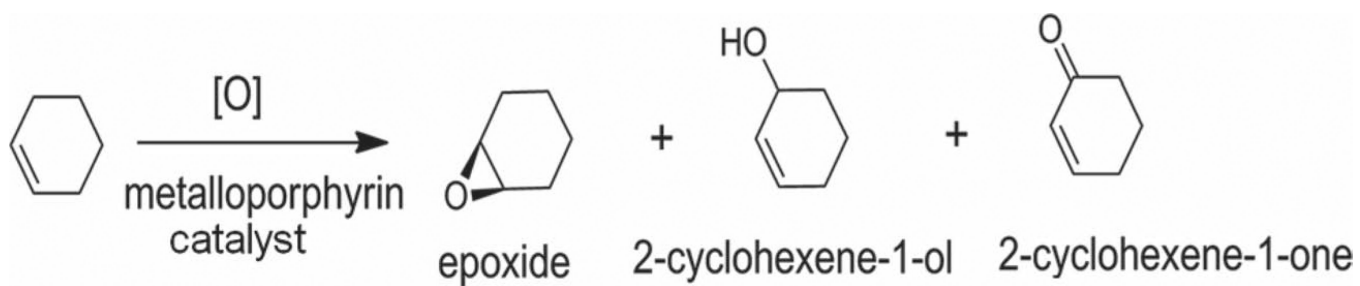


Figure 2.

(A) TEM image of a cluster of four ONP of Fe(III)TPPF₈₄ on a carbon-coated copper grid, (B) where the 15–20 nm diameter ONP are outlined and indicated by arrows. (C) The scheme shows a cartoon of the hierarchical organization of one ONP and a few of the many 2–3 nm subdomains, each consisting of 2–4 metalloporphyrins. The histogram at the bottom shows the size distribution of the small subdomains contained within the ONP.

**Scheme 1.**

Preparation of Fe(III)TPPF₈₄ from Fe(III)TPPF₂₀: (i) DMF/DIPEA under N₂ at rt. for 2 h. Addition of water with 2% triethyleneglycol monomethylether to a THF solution of the catalytic porphyrin forms the ONP.



Scheme 2.
Oxidation of cyclohexene using metalloporphyrin catalysts.

Table 1

Fe(III)/TPPF₈₄ catalysis of cyclohexene oxidation.

Solution ^{a)} or ONP ^{b)}	Conditions	% epoxide	% enol	% enone	TON	Comments
Solution	125 mL O ₂	16	29	55	158	36% porphyrin left
Solution	125 mL O ₂	20	27	53	147	72 h, no porphyrin left
Solution	125 mL O ₂ , 1.73 atm	13	32	55	129	No porphyrin left
Solution	125 mL O ₂ , 40 °C	8	35	57	140	No porphyrin left
Solution	125 mL O ₂ , 50 °C	6	38	56	123	No porphyrin left
ONP	125 mL O ₂	<1	29	70	670	26% porphyrin left
ONP	125 mL O ₂	<1	32	67	350	72 h, no porphyrin left
ONP	125 mL O ₂ , 1.73 atm	<1	31	68	305	No porphyrin left
ONP	125 mL O ₂ , 40 °C or 50 °C	X	X	X	X	No porphyrin left

Reactions were run at room temperature and 1 atm for 24 h unless noted;

^{a)} Solution reactions: 0.4 mL (1×10^{-3} M, 4×10^{-7} mol of porphyrin) of catalyst was mixed with 2.5 mL of methanol: acetonitrile (1:3) and 0.2 mL of cyclohexene to a final concentration of 0.13×10^{-3} M, 125 mL of O₂, porphyrin: cyclohexene: O₂ = 1:4800:13000 was used;

^{b)} ONP reactions with O₂: 15–20 nm diameter ONP suspension (2.5 mL, 70×10^{-6} M, 1.75×10^{-7} mol of porphyrin) mixed with cyclohexene (0.2 mL) and O₂² (125 mL); porphyrin: cyclohexene: O₂ = 1:11300: 29000. TON = mol/products/mol porphyrin has an error of $\pm 5\%$. Products were extracted into CH₂Cl₂ and analyzed by using an Agilent 5975 series GC – MS. Control reactions: neither H₂O₂ nor O₂ react directly with cyclohexene under these conditions (Table S1, Supporting Information).